

Reconstruction and Visualization of 3D Models of Colonic Surface

Lichan Hong*, Zhengrong Liang⁺*, Ajay Viswambharan⁺, Arie Kaufman^{*+}, and Mark Wax⁺

*Department of Computer Science ⁺Department of Radiology

Center for Visual Computing

State University of New York at Stony Brook, Stony Brook, NY 11794

Abstract

This paper presents an innovative technology called *3D virtual colonoscopy*, which incorporates several advanced visualization techniques to enable the physician to virtually examine the inner surface of the entire colon for identifying and inspecting colonic polyps. We first describe our unique process of acquiring and reconstructing a patient's colon model, followed by the novel visualization algorithms that we have developed to provide automatic planned navigations as well as interactive guided navigations inside the colon. Finally, we present our experimental results on a simulated pipe phantom, the Visible Human data set, and patient data.

I. INTRODUCTION

Cancer of the colon and rectum is the second leading cause of cancer deaths in the United States [14],[16]. Every year, there are approximately 150,000 new cases of colorectal cancer diagnosed, with a much larger number of colon screening examinations performed. Among men, the annual incidence of colorectal cancer ranks third behind lung and prostate cancer, and in women it is the second only to breast cancer. At age 50, an American man or woman has a 1 in 20 probability of developing cancer of the colon or rectum and a 2.5% likelihood of dying of this disease. Unfortunately, colon cancer is most often discovered after the patient has developed symptoms. Such high prevalence of colon cancer requires a cost-effective and patient-comfortable screening procedure to diagnose the disease at an earlier stage, so that an immediate treatment will improve the survival ratio of the patients.

Colon polyps that are 5mm or larger are considered to be clinically significant, since they have high probability of being malignant [13],[19]. Detection and removal of small polyps can totally eradicate the disease. Currently, for colorectal cancer screening, there are several diagnostic procedures, such as digital rectal examination, fecal occult blood test, flexible sigmoidoscopy, barium enema, and optical colonoscopy. These diagnostic tests differ greatly with respect to safety, ease of performance, degree of patient compliance, expense, and diagnostic accuracy (both sensitivity and specificity). Among these methods, only optical colonoscopy and barium enema can be used to examine the entire colon.

Optical colonoscopy, an invasive procedure utilizing a fiber optical probe, presents a small risk of perforation. It also requires intravenous sedation and takes approximately 40 to 60 minutes to perform. Frequently, due to either technical

difficulties or patient discomfort, the proximal colon can not be fully examined. Furthermore, the cost of optical colonoscopy is relatively high, ranging from \$1,300 to \$1,900. Alternatively, single/double contrast barium enema, although less expensive (approximately \$400) and noninvasive, requires a good deal of patient positioning and physical cooperation from the patient when X-ray radiographs of the colon are taken at different views. Diagnostic results vary according to the technical quality of this modality and the experience of the interpreter. While some investigators claim that barium enema can be as sensitive and specific as optical colonoscopy, others have reported that the sensitivity achieved with barium enema can be as low as 78% in detection of polyps in the range of 5mm to 20mm in diameter [12].

An innovative procedure, which utilizes computer technology to virtually examine the inner surface of the entire colon based on CT images of the patient's abdomen, has promising potential to improve the sensitivity and specificity of the diagnosis with fewer complications and patient discomfort [4],[5],[10],[18],[22]. In this paper, we present such a procedure, called *3D virtual colonoscopy*, which we have been independently developing in the past few years. First, in Section II we describe the medical routine used to acquire and reconstruct the three-dimensional (3D) model of the patient's colon. Then, in Section III we propose two novel algorithms for the visualization of the 3D colonic surface. These techniques enable the physician to automatically "fly-through" the inside of the colon to obtain a general overview of the inner surface, as well as interactively navigate through the colon to study a particular structure in detail. Finally, in Section IV we present our testing results on a simulated pipe phantom, the Visible Human data set, and patient data.

II. DATA PREPARATION

The first phase of 3D virtual colonoscopy is to prepare the colon model so that it can be later studied and explored with the visualization techniques. This involves four steps. First, the patient's colon is cleansed, similarly to what is required for an optical colonoscopy. Second, air is inflated into the colon to produce better contrast between the lumen and the colonic wall. In the third step, a spiral CT scan of the patient's abdomen is taken. In the fourth step, the acquired CT images are reconstructed first into thin 2D slices and subsequently into a 3D volume.

Specifically, the cleansing process requires that, starting two days prior to the CT scanning, the patient drinks 100cc of liquid barium with each meal. In addition, on the evening prior to the

day of scanning, the patient takes a standard colonic cleansing routine by drinking one gallon of Golytely solution. After the patient has arrived at the CT scanning suite, a small bore rectal catheter is placed into the rectum and approximately 1,000cc air is pumped into the colon. The colon, when distended with air, yields excellent contrast between the wall and the lumen. Next, while the patient holds his or her breath, a spiral CT scan of 5mm thickness utilizing 1:1 pitch and 40cm field-of-view is performed over the patient's abdomen. This scan, which takes about 30 to 45 seconds, starts from the level of the top of the splenic flexure of the colon to the rectum based on the landmarks obtained from the scout image. The acquired CT data are then reconstructed into transaxial slices spaced 1mm apart. This usually results in several hundred 2D images of 512×512 pixels, which are subsequently assembled into a 3D volumetric data of size 100 to 250 Mbytes.

III. VISUALIZATION TECHNIQUES

A. Automatic Planned Navigations

After the volumetric representation for the patient's abdomen has been obtained, a fly-through animation along the inside of the colon can be generated to provide a general overview of the inner surface. This is accomplished by moving a virtual camera along a pre-determined flight path, essentially from one end of the colon to the other end of the colon (we call such virtual fly-throughs *planned navigations*).

In general, to produce a planned navigation, one needs to first find a set of *key points* and determine the camera direction at each key point [2]. The fly-through animation is subsequently generated with the camera parameters computed at these key points, as described later in this section. To obtain the camera locations and directions for the key points, one can go through the process of *manual specifications* (e.g., [18]), which could be rather tedious and time-consuming because the volumetric data set is very large. Another option is to utilize the computer to *automatically* calculate the information at the key points [5],[10]. In Lorensen et al.'s algorithm [10], a wavefront propagation scheme coupled with a steepest descent method are used to automatically construct a flight path from a user-specified start point to a user-specified target point. Each voxel on the flight path essentially corresponds to a key point for the fly-through animation. Unfortunately, in some cases the flight path is too close to one side of the colonic surface, yet too far away from another side of the surface, resulting in a highly unbalanced field of view in the fly-through animation. Furthermore, it is unclear how the camera direction at each key point is determined in the algorithm.

We have recently designed a new algorithm [5], with the aim of automatically generating a planned navigation which is smooth with a balanced field of view. From our experiments, we have found that to obtain a balanced field of view, the *center-line* (or *skeleton*) of the colon is an appealing choice for the flight path. This center-line can be calculated with a technique similar to the process of "peeling an onion" [15], as demonstrated in Fig. 1 (for simplicity, a 2D example is used here; our algorithm actually works in 3D). More specifically,

at first two "blocking walls" are specified (unnecessary if examination of the whole colon is desired), defining a region

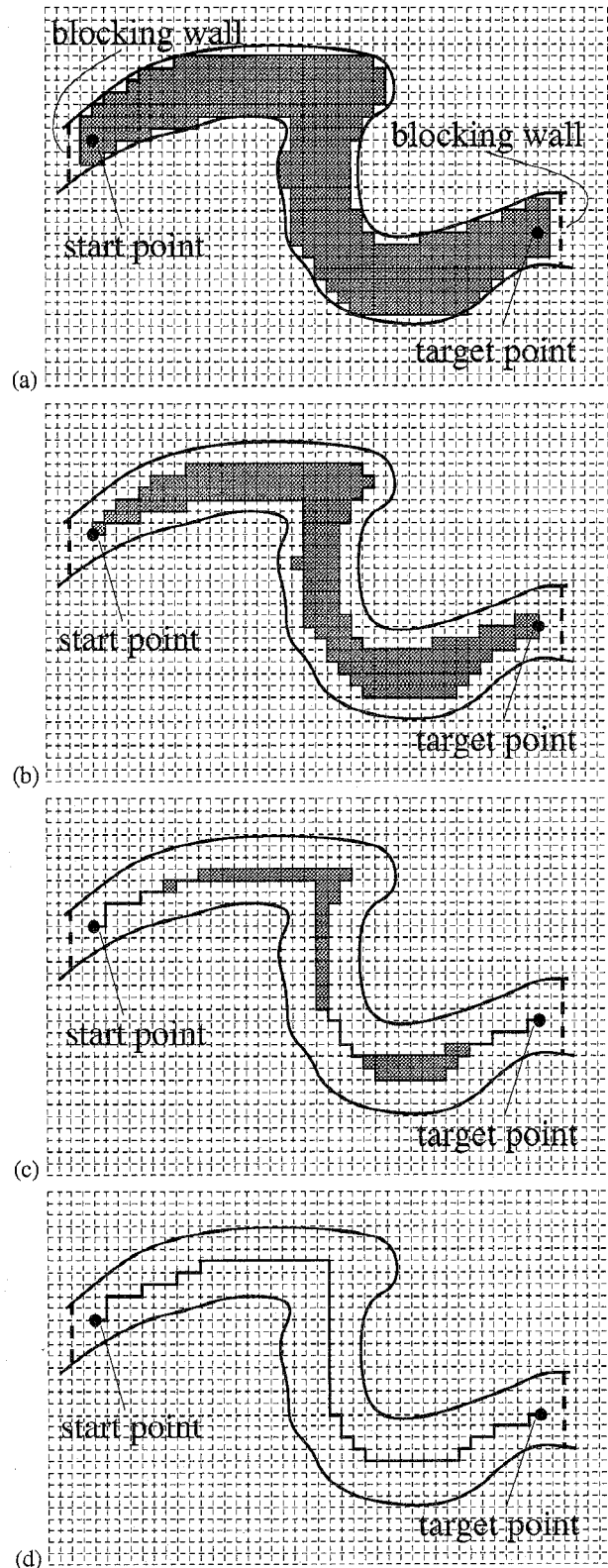


Fig. 1 The process of extracting the center-line of the colon.

of interest enclosed by the colonic surface and the blocking walls. Next, the start point and the target point of the flight path are selected. From that point on, the computer takes over and calculates the center-line of the extracted sub-volume (shown

in dark grey in Fig. 1a) by peeling off the outermost layer of the sub-volume one-by-one until there is only one layer of voxels left (see Figs. 1a to 1d). Each voxel on the center-line is then used as a key point for the fly-through animation.

To determine the camera direction at a key point, instead of simply using the vector which points from the current key point towards the next key point on the flight path, we utilize some key points which are further down along the flight path. For example, as illustrated in Fig. 2, to decide the camera direction at key point A , we examine all the key points between B and C for their visibility from A . If all of them are visible from point A (i.e., the line segment connecting point A and the tested point does not intersect with the surface), we use a vector between AB and AC as the camera direction for point A . Otherwise, we move B and C one voxel closer to point A along the flight path, and perform the testing again. This process is repeated until the camera direction for key point A is decided.

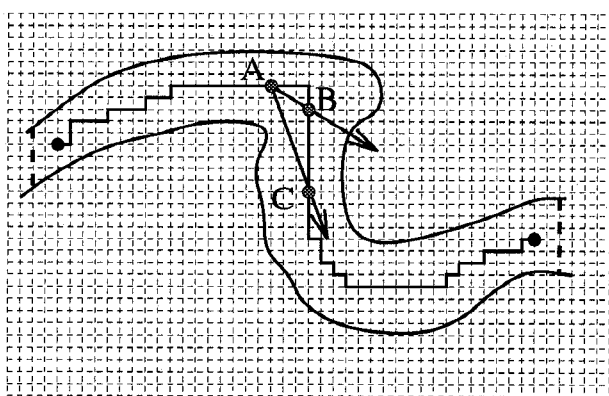


Fig. 2 Computing the camera direction at key point A .

After the camera locations and directions at the key points have been calculated, the camera parameters for the intermediate frames are computed using an interpolation scheme such as cubic splines [8]. Because the animation is generated off-line, high-quality rendering (e.g., volumetric ray tracing [20]) is used to produce each frame.

B. Interactive Guided Navigations

Automatic planned navigation relieves the user from manually specifying the camera parameters for the key points and provides an overview of the colonic surface. However, in many cases, planned navigation is not enough. For example, during a planned navigation, an irregularity on the colonic wall has been observed and further study is required. This kind of detailed study usually involves observing the suspicious structure from different angles, measuring the location as well as size of the abnormality, and even examining the density values under the surface. In this section, we mainly focus on how to enable the physician to interactively navigate inside the colon.

Generally speaking, to obtain an interactive navigation, there are two important concerns which need to be addressed: camera control and rendering speed. Camera control specifies how the camera is manipulated and moved inside the colon to achieve the visualization, while interactive rendering rate is crucial for this technology to be accepted by the physician. In

the following, we describe how the camera is controlled in the navigation and how interactive rendering speed is achieved.

1) Camera Control

There are two extreme camera control models for navigating within a 3D virtual environment [1]. One pre-determines the navigation path for the camera, as demonstrated in planned navigations. The other extreme gives the user full control of the camera. That is, the user is asked to directly manipulate the camera location and direction, using either 2D or 3D input devices. However, for interactive navigations inside the colon, it may be cumbersome for the physician to be fully responsible for the control of the camera. This is because, even with advanced 3D input devices, it could be difficult for the physician to obtain a satisfactory tour of the colonic surface by controlling the camera. In addition, it would be rather tedious and tiring for the physician to specify where to go and what to see at each step of the navigation. Furthermore, the camera may be unintentionally moved out of the colon.

To prevent the physician from taking full responsibility of controlling the camera while allowing certain influences over the movement of the camera, we have recently developed an interactive guided navigation technique [6]. The objective was to move the camera automatically as in planned navigation when there is no user input, and be able to manipulate the camera in an intuitive way when an influence is desired. Additionally, the camera control model should also guarantee that the camera never penetrates the colonic wall. For this purpose, the colonic interior is simulated with a potential field and a set of kinematic equations is used to calculate the movement of the camera. As a result, the inside of the colon is like a "river" (or more exactly a "tunnel"), with the water running from the user-specified start point towards the user-specified target point, and the camera is mounted on a "submarine" whose movement is governed by the flow of the water as well as the motor of the submarine.

More specifically, the potential value $P(\mathbf{x})$ for a voxel \mathbf{x} inside the colon is computed as a function of three distance fields: (1) distance from the target point $d_t(\mathbf{x})$, (2) distance from the colonic center-line $d_c(\mathbf{x})$, and (3) distance from the colonic surface $d_s(\mathbf{x})$. The function is in the form of

$$P(\mathbf{x}) = C_1 d_t(\mathbf{x})^\mu + C_2 \left(\frac{d_s(\mathbf{x})}{d_c(\mathbf{x}) + d_s(\mathbf{x})} \right)^{-\nu} \quad (1)$$

where C_1 , C_2 , μ , and ν are constants interactively chosen by the physician. Consequently, there are high potential values far away from the target point, and low potential values close to the target point. Similarly, there are high potential values near the surface, and low potential values close to the center-line. In fact, to prevent the camera from being moved out of the colon, sufficiently large potential values are used in those areas proximity to the surface.

In addition, the submarine is modeled as two particles connected by an unextensible, weightless rod (see Fig. 3). The positions of the particles are given as \mathbf{x}_1 and \mathbf{x}_2 , and the particles are assumed to have the same mass m . A camera is attached at particle \mathbf{x}_1 and the vector $\mathbf{x}_2 - \mathbf{x}_1$ is used as the camera direction. This submarine (and essentially the camera)

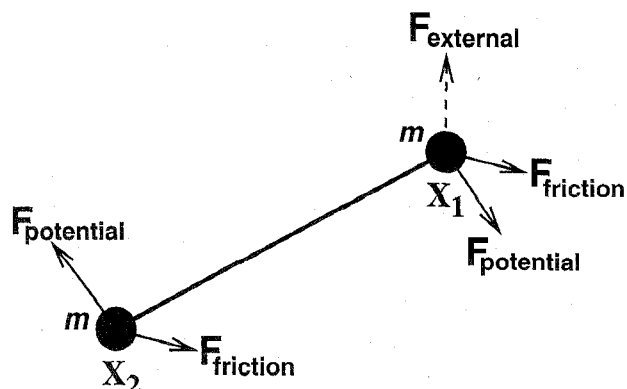


Fig. 3 The submarine model for interactive navigations.

performs translations as well as rotations as the two particles are affected by the potential field forces $F_{potential}(\mathbf{x})$, friction forces $F_{friction}(\mathbf{x})$, and optional external forces $F_{external}(\mathbf{x})$. We compute

$$F_{potential}(\mathbf{x}) = -m\nabla P(\mathbf{x}) \quad (2)$$

and

$$F_{friction}(\mathbf{x}) = -k\dot{\mathbf{x}}, \quad (3)$$

where $\nabla P(\mathbf{x})$ is the gradient of $P(\mathbf{x})$ at point \mathbf{x} , k the friction coefficient, and $\dot{\mathbf{x}}$ the particle's velocity. $F_{external}(\mathbf{x})$ is specified by clicking a 2D mouse on a pixel of the display screen. Based on the geometry of the viewing frustum, the 3D location of the screen pixel clicked on by the mouse is computed. The direction of $F_{external}(\mathbf{x})$ is then assigned as a unit vector pointing from the camera \mathbf{x} to the screen pixel. The magnitude of $F_{external}(\mathbf{x})$ is a parameter which can be interactively modified by the physician. Applying $F_{external}(\mathbf{x})$ results in bringing the camera towards the area pointed by the mouse.

2) Interactive Rendering

Interactive rendering speed is also very important in guided navigations. This is because low rendering rate causes temporal aliasing and hinders the illusion of immersion (the feeling that the physician is working in a *real* environment). Moreover, low rendering rate makes it difficult for the physician to control the camera, because of the response latency between the moment the physician applies an external force and the moment he or she sees the result of that action.

Since the data set that we have obtained from the scanning is inherently volumetric, to generate the images on-the-fly during the navigation, volume rendering [7] seems to be a natural choice. Unfortunately, even with a commercially available high-end graphics workstation (e.g. an SGI InfiniteReality), none of the current volume rendering methods is fast enough to deliver high-resolution (e.g., 640×480), high-quality images at interactive speed. To overcome this problem, Vining et al. [23] focused on visualizing only a small portion of the entire colon at a time. While in Reed et al. [17], before the navigation, a large number of images seen from several viewing angles at a set of locations inside the colon are pre-rendered using an approximate volume rendering algorithm and stored in the memory. During the navigation, the image for a specific camera location and direction is approximated by interpolating from those pre-generated images.

To visualize the entire colon while preserving the image quality, we use the Marching Cubes algorithm [9] to extract a triangle mesh of isodensity from the volumetric data and later render the triangles with graphics hardware. For such a huge data set of several hundred Mbytes, a brute-force Marching Cubes algorithm usually produces an enormous amount of triangles, which requires several minutes to render on a high-end graphics workstation. Our objective was to reduce the number of triangles to a certain degree before they are delivered to the graphics engine, in order to achieve interactive speed on a high-end graphics workstation. Early in our work we noted that although the abdomen volume includes information about other organs, we only need to keep the triangles representing the colonic surface because this is what we want to visualize. By excluding those triangles that are not part of the colonic surface, we have substantially reduced the number of triangles.

Another property that we have exploited is the twisted nature of the colon. More specifically, given a particular camera location and direction inside the colon, what we are able to see is usually only a small fraction of the entire colonic surface. This means that, to generate an image at a specific moment, we do not need to render all the surface triangles because most of them are not visible to the camera anyway. This essentially becomes a visibility problem [3],[11],[21]. Unfortunately, these existing algorithms are either too slow or tailored to other applications such as architectural walk-throughs. To address this issue, we have developed a special visibility algorithm [6] by subdividing the colon into a set of small sections, called cells, based on the center-line of the colon. Then, by conservatively estimating the potentially visible set of cells from the camera using the depth buffer in the graphics hardware, we have drastically reduced the number of triangles submitted for rendering. Consequently, with these innovations of focusing on the inner surface and computing the visibility, we are able to navigate through a typical colon model at about 15 frames/second on an SGI InfiniteReality.

IV. EXPERIMENTAL RESULTS

We have tested our algorithms on several data sets. These include a simulated plastic pipe phantom data, the Visible Human data, and ten patient data.

The objective of the pipe simulation was to see how well we could detect the presence and characteristics of colonic polyps. In this simulation, we looped a plastic pipe inside a water tank. The pipe had a radius of $20mm$ and its surface had corrugated and smooth segments. To simulate colonic polyps, we attached three rubber cylinders to the inner surface of the pipe. The lengths of these three cylinders were $7mm$, $5mm$, and $3mm$, respectively, and the diameters were $5mm$ for all cylinders. With a GE HighSpeed CT in the helical mode, we obtained a volumetric data set of $512 \times 512 \times 107$. Fig. 4 shows an image generated in a planned navigation inside the pipe. The three simulated polyps are clearly visible from the figure.

In our second study, we used the Visible Male data, which is available from the National Library of Medicine (for detailed information about the data set, see the web page at

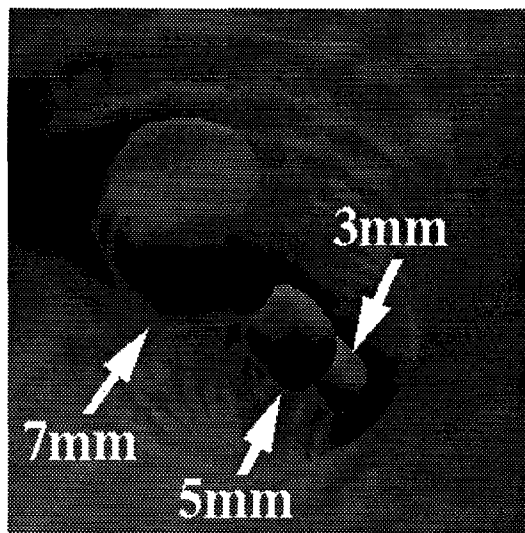


Fig. 4 An image from a planned navigation inside the pipe showing the three simulated polyps.

<http://www.nlm.nih.gov/research/visible>). We focused on the physical cross-sections, from slice 1595 to slice 1848. Due to memory limitations, each slice of the physical cross-sections was down-sampled from the original resolution of 2048×1216 to 683×406 . For the navigations, the 24-bit color slices were converted into 8-bit grayscale, segmented, and reconstructed into a volumetric format. Fig. 5 is an image from an interactive

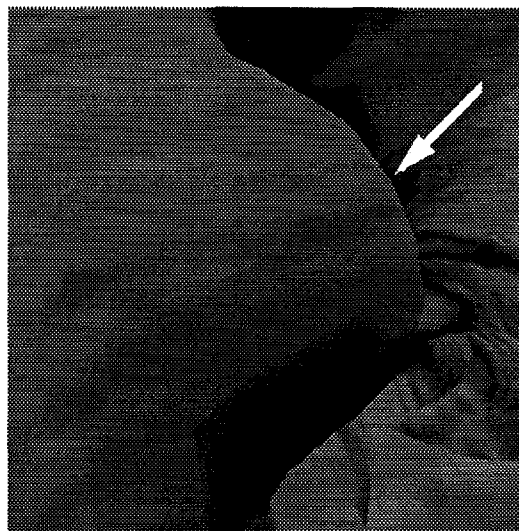


Fig. 5 An image from an interactive navigation through the colon of the Visible Male depicting an abnormality of size 5mm on the surface.

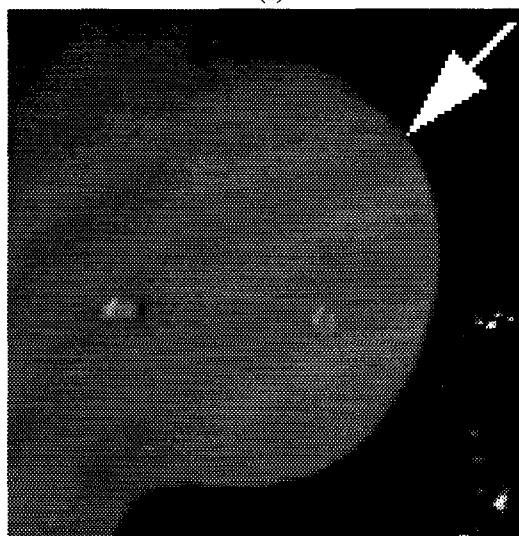
navigation through the colon of the Visible Male, where an abnormality of size 5mm on the colonic surface of the Visible Male was discovered.

Due to the encouraging results that we had obtained from the two experiments, we proceeded with patient studies. After the approval of patient studies by the University Hospital Committee on Research Involving Human Subject, ten volunteers have been recruited. For the ten patient cases, abnormalities discovered in planned navigations as well as interactive navigations have been documented and are currently being evaluated against the results of the optical colonoscopy,

which was performed by gastroenterologists immediately following the CT scans. In Fig. 6 we compare a diagnostic result of virtual colonoscopy with that of optical colonoscopy.



(a)



(b)

Fig. 6 (a) A polyp of size 8mm discovered in virtual colonoscopy. (b) The corresponding polyp of (a) confirmed by optical colonoscopy.

V. CONCLUSIONS

In this paper we have reported a computerized procedure for the screening of colorectal cancer. Our procedure has the following unique properties. First, as compared with optical colonoscopy and barium enema, the data acquisition process is noninvasive, faster, and cost effective. Second, the planned navigation provides a general overview of the colon, while the interactive navigation allows the physician to study particular abnormalities in detail. The visualization provides the physician with unlimited viewing angles for examining the abnormalities as long as desired and as many times as required. Finally, when necessary, the physician can also employ volume rendering as well as virtual biopsy to peer inside the polyps. Since the abdomen is represented in a volumetric format, this feature becomes rather easy to achieve and can be very helpful

for the diagnosis of colonic polyps. If polyps are discovered in virtual colonoscopy, the patient will be referred to optical colonoscopy for final decision and physical biopsy.

Evaluations of 3D virtual colonoscopy on clinical cases are underway. Also, we are currently calibrating the visualization techniques and incorporating more volume rendering functionalities to help the physician to differentiate remaining stool from polyps by examining the internal characteristics of the abnormalities. In the future, we plan to investigate other contrasting agents for automatically distinguishing stool from polyps. Finally, our techniques are being extended to examine other human organs (e.g., blood vessels) where traditional medical procedures are difficult to perform.

VI. ACKNOWLEDGMENTS

This research has been supported by the Center for Biotechnology of New York State and E-Z-EM Inc. The Visible Male data set is courtesy of the National Library of Medicine and the Visible Human Project. We thank Shigeru Muraki, Taosong He, Dirk Bartz, and Yi-Chih Wei for their valuable contributions to this project.

VII. REFERENCES

- [1] F. Brooks, "Walkthrough - A Dynamic Graphics System for Simulating Virtual Buildings," *Proc. ACM Workshop on Interactive 3D Graphics*, 1986, pp. 9-21.
- [2] J. Foley, A. Van Dam, S. Feiner, and J. Hughes, "Computer Graphics: Principles and Practice," *Addison-Wesley*, 1990.
- [3] N. Greene, M. Kass, and G. Miller, "Hierarchical Z-Buffer Visibility," *Computer Graphics (Proc. ACM SIGGRAPH '93)*, pp. 231-236.
- [4] A. Hara, C. Johnson, J. Reed, D. Ahlquist, H. Nelson, R. Ehman, C. McCollough, and D. Ilstrup, "Detection of Colorectal Polyps by Computed Tomographic Colography: Feasibility of a Novel Technique," *Gastroenterology*, vol. 110, 1996, pp. 284-290.
- [5] L. Hong, A. Kaufman, Y. Wei, A. Viswambharan, M. Wax, and Z. Liang, "3D Virtual Colonoscopy," *Proc. IEEE Biomedical Visualization Symposium*, 1995, pp. 26-32.
- [6] L. Hong, S. Muraki, T. He, and A. Kaufman, "Physically-Based Interactive Navigation," *Technical Report TR.96.01.09, Computer Science Department, SUNY at Stony Brook, January 1996*.
- [7] A. Kaufman, "Volume Visualization," *IEEE Computer Society Press*, 1991.
- [8] D. Kochanek and R. Bartels, "Interpolating Splines with Local Tension, Continuity, and Bias Control," *Computer Graphics (Proc. ACM SIGGRAPH '84)*, pp. 33-41.
- [9] W. Lorensen and H. Cline, "Marching Cubes: A High Resolution 3D Surface Construction Algorithm," *Computer Graphics (Proc. ACM SIGGRAPH '87)*, pp. 163-169.
- [10] W. Lorensen, F. Jolesz, and R. Kikinis, "The Exploration of Cross-Sectional Data with a Virtual Endoscope," in *R. Satava and K. Morgan (eds.), Interactive Technology and New Medical Paradigm for Health Care*, IOS Press, 1995, pp. 221-230.
- [11] D. Luebke and C. Georges, "Portals and Mirrors: Simple, Fast Evaluation of Potential Visible Sets," *Proc. ACM Symposium on Interactive 3D Graphics*, 1995, pp. 105-106.
- [12] C. Morosi, G. Ballardini, and P. Pisani, "Diagnostic Accuracy of the Double-Contrast Enema for Colonic Polyps in Patients with or without Diverticular Disease," *Gastrointest Radiology*, vol. 16, 1991, pp. 346-347.
- [13] T. Muto, H. Bussey, and B. Morson, "The Evolution of Cancer of the Colon and Rectum," *Cancer*, vol. 36, 1975, pp. 2251-2270.
- [14] M. O'Brien, S. Winawer, and A. Zauber, "The National Polyp Study: Patient and Polyp Characteristics Associated with High-Grade Dysplasia in Colorectal Adenomas," *Gastroenterology*, vol. 98, 1990, pp. 371-379.
- [15] T. Pavlidis, "Algorithms for Graphics and Image Processing," *Computer Science Press*, 1982.
- [16] J. Potter and M. Slattery, "Colon Cancer: A Review of the Epidemiology," *Epidemiology Review*, vol. 15, 1993, pp. 499-545.
- [17] J. Reed, A. Hara, and C. Johnson, "Interactive Diagnostic, Low-Cost CT Colography (Virtual Endoscopy): Feasibility of a Rendering Algorithm," *Proc. Annual Conference of Radiological Society of North America (RSNA)*, 1996, pp. 252.
- [18] G. Rubin, C. Beaulieu, V. Argiro, H. Ringl, A. Norbash, J. Feller, M. Dake, R. Jeffrey, and S. Napel, "Perspective Volume Rendering of CT and MR Images: Applications for Endoscopic Imaging," *Radiology*, vol. 199, May 1996, pp. 321-330.
- [19] B. Simons, A. Morrison, R. Lev, and W. Verhoek-Oftendahl, "Relationship of Polyps to Cancer of the Large Intestine," *Journal of National Cancer Institute*, vol. 84, 1992, pp. 962-966.
- [20] L. Sobierajski and A. Kaufman, "Volumetric Ray Tracing," *Proc. ACM Symposium on Volume Visualization*, 1994, pp. 11-18.
- [21] S. Teller and C. Sequin, "Visibility Preprocessing For Interactive Walkthroughs," *Computer Graphics (Proc. ACM SIGGRAPH '91)*, pp. 61-69.
- [22] D. Vining, D. Gelfand, R. Bechtold, E. Scharling, E. Grishaw, and R. Shifrin, "Technical Feasibility of Colon Imaging with Helical CT and Virtual Reality," *Annual Meeting of American Roentgen Ray Society*, 1994, pp. 104.
- [23] D. Vining, D. Stelts, G. Hunt, D. Ahn, Y. Ge, and P. Hemler, "Technical Improvements in Virtual Colonoscopy," *Proc. Annual Conference of Radiological Society of North America (RSNA)*, 1996, pp. 524-525.